Modeling of Human Welder Response to 3D Weld Pool Surface: Part II – Results and Analysis

This paper is devoted to the design of dynamic experiments as well as use of the resultant data to model and analyze a welder's dynamic responses

BY W. J. ZHANG AND Y. M. ZHANG

ABSTRACT

Understanding and modeling a human welder's responses to a 3D weld pool surface may help develop intelligent welding robotic systems and train welders faster. In this first effort on modeling a human welder's behavior, a novice welder's adjustment on the welding current as a response to the 3D weld pool surface as characterized by its width, length, and convexity is studied. The first part of the paper used an innovative machine vision system to measure/record in real time the specular 3D weld pool surface from experiments and conducted preparation experiments to reduce the inconsistencies in the welder's responses as well as determine the welder's delay and time intervals of the process response. In this part of the paper, experiments are designed to produce random changes in the weld pool using random welding speeds in order to model the response of the welder to a dynamic weld pool surface. The fluctuating weld pool surface and welder's adjustments on the welding current are recorded. Through the least squares algorithm, various models with different structures are identified to correlate the current adjustment to the 3D weld pool surface. It is found that the human welder's responses are not only related to the 3D weld pool surface but also rely on the welder's previous adjustments. The resultant model has been verified by further experiments for its effectiveness in predicting the welder's responses.

Introduction

The goal of this study on human welder behaviors is to establish a dynamic model for a novice welder's adjustment on the welding current in response to the observed 3D weld pool surface during a complete-joint-penetration process. That is to establish a model that correlates the welder's responses (model output) to the characteristic parameters (inputs) of the 3D weld pool surface. In Part 1 of this paper (Ref. 1), the principle of a human welder's behavior was analyzed. A vision-based sensing system was used to record in real time the human welder's responses and the 3D weld pool geometry characterized by three parameters — the length, width, and surface convexity of the weld pool. Preparation experiments were designed and conducted to improve the welder's response consistency and determine the welder's response time interval as determined by the transition time and response delay.

With the improved consistency and knowledge about the transition time and welder response delay, the foundation to model the welder's responses were established in Part 1 of the paper. However, dynamic variations in the welding speed need to be applied to generate more dynamic weld pools in order to accurately identify and model the welder's responses to the dynamic weld pool surface. To this end, as the second part of the study, this paper is devoted to the design of dynamic experiments as well as use of the resultant data to model and analyze a welder's dynamic responses.

The design of the dynamic experiments is presented in the experimental method section. In the identification method section, these methods are briefly introduced. The modeling of the welder's responses and the analysis of resultant models are detailed in the modeling and static response analysis parts of the modeling of response to weld pool surface section, respectively. In the improved modeling and understanding of human welder response section, based on the analysis for the modeling of response to weld pool surface section, the welder's previous responses are included to improve the response model. To verify the resultant model, further experiments were conducted, and the verification of the model using the data from those experiments is detailed in the verification and discussion section. The conclusion is drawn in the final section.

KEYWORDS

Human Welder's Behavior Modeling
3D Weld Pool Surface
Gas Tungsten Arc Welding (GTAW)

Experimental Method

In order to identify the model of the welder's dynamic responses to the 3D weld pool surface, dynamic experiments with random welding speed variations will be conducted. These dynamic experiments should be similar to those conducted in the adaptation process. To this end, there are five welding speeds to be used in the dynamic experiments, as follows: 1, 1.25, 1.5, 1.75, and 2.0 mm/s. Hence, for each experiment, the welding speed is randomly changed among the five welding speeds. To determine how frequently the speed change should be made, the average transition time of the welding process can be used as a reference. From Part I, the average transition time is 8.7 s,

W. J. ZHANG and Y. M. ZHANG (ymzhang@engr.uky.edu) *are with the Institute for Sustainable Manufacturing and Department of Electrical and Computer Engineering, University of Kentucky, Lexington, Ky.*

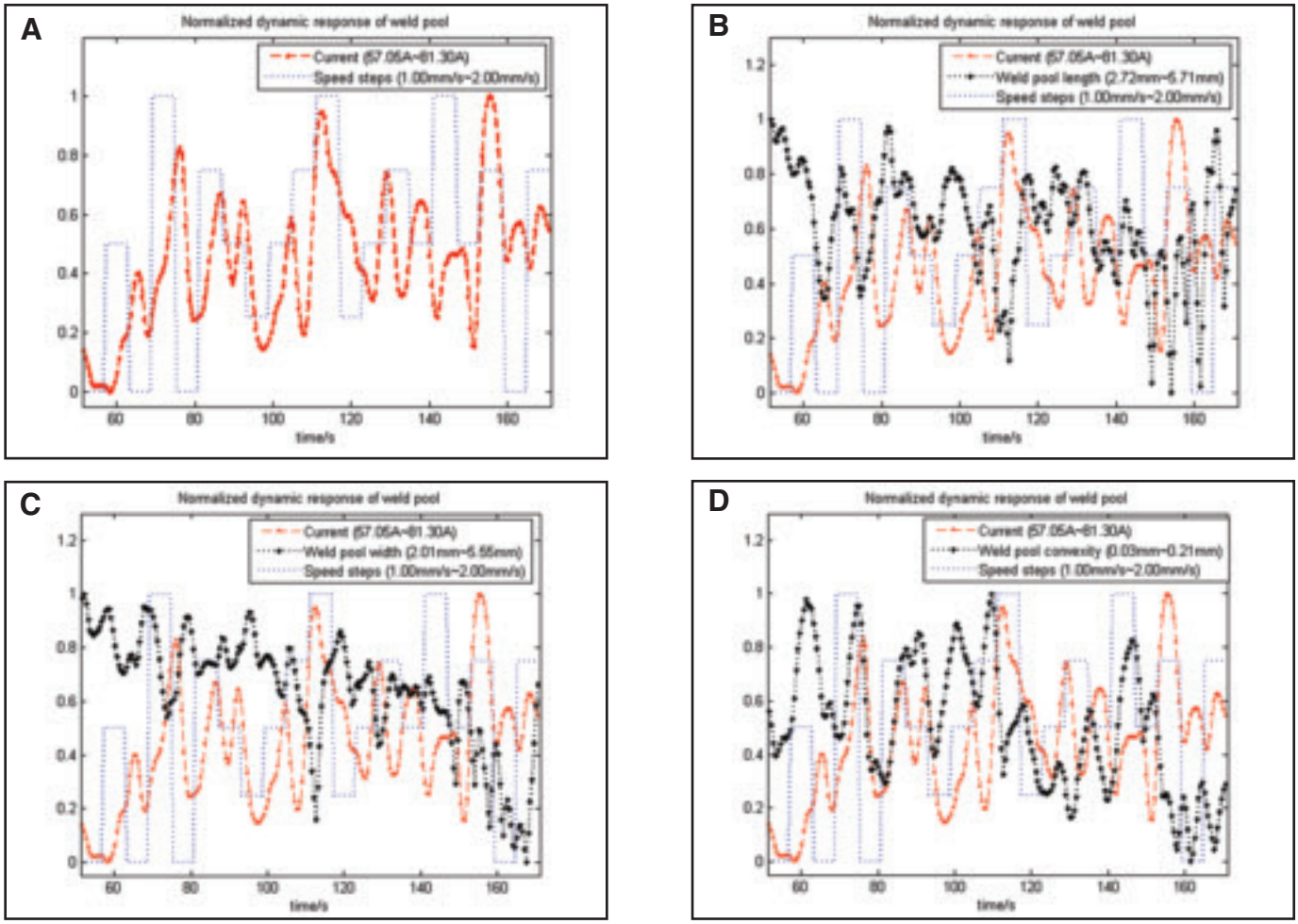

Fig. 1 — Identification experiment. A — Current and speed; B — length, current, and speed; C — width, current, and speed; D — convexity, current, and speed. All variables are plotted using the normalized scale. The range for each variable is given in each plot and corresponds to [0, 1] in the normalized scale.

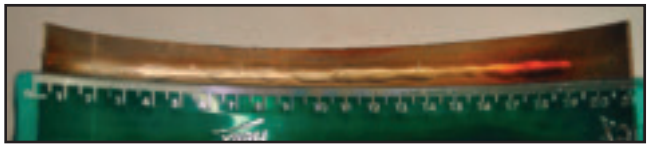

Fig. 2 — Backside weld bead from the identification experiment.

including the time delay of the welder, the welder's response time, and the settling time of the weld pool. In this sense, the speed change interval should be shorter than the transition time, since it is not necessary for each speed to last till the weld pool fully resumes its steady state. Therefore, in this study, the time interval for each change is set to be 6 s.

Each experiment has two periods. The constant speed period and random speed period use a constant welding speed and a randomly changing welding speed, respectively. The purpose of the constant speed period is to allow the human welder to bring the welding process to the desired complete-joint-penetration state, and the random speed period is to produce the dynamic weld pool for the human welder to respond. The duration of the constant speed period is set at 18 s, long enough to establish a steady state for the welding process. The duration for the random speed period is 120 s. The arc length is set at the same constant in each experiment in [2, 5 mm], i.e., 2, 3, 4, and 5 mm. Other experimental settings are shown in Table 1 in Part I of this paper.

The data from one experiment will be used to identify the model. This will then be verified using data from all other experiments. The arc length used in the identification experiment that produces the data to identify the model is 3 mm. The results of the identification experiment are shown in Fig. 1. It is found in Fig. 1A that the current controlled by the human welder basically follows the tendency of the welding speed changes. Since the weld pool dimension varies significantly as the welding speed fluctuates, the human welder adjusts the current afterward. Figure 1B and C show that the tendency of the current adjustment is appropriately opposite to the length and width fluctuation. The waveform of convexity as shown in Fig. 1D basically coincides with the current variation. The variations in the weld pool surface geometry and the current indicate that the human welder reduces the current as the weld pool length or width raises, and increases it as the weld pool

Table 1 — Resultant Models of the Human Welder Response with One Input

Inputs	σ	*r*	Models
Length	1.9023	0.132	$\Delta i_k = -0.070 l_{k-4} + 0.2037 l_{k-5} + 0.2968 l_{k-6} - 1.9215$
Width	1.9068	0.1	$\Delta i_k = -0.2287 w_{k-3} + 0.1376 w_{k-4} + 0.2819 w_{k-5} - 0.7828$
Convexity	1.8222	0.32	$\Delta i_k = 39.3114 h_{k-3} + 3.2639 h_{k-4} - 38.3469 h_{k-5} - 0.4715$

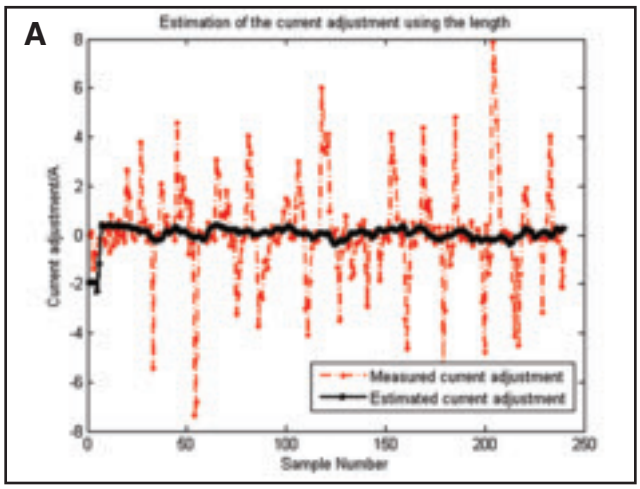

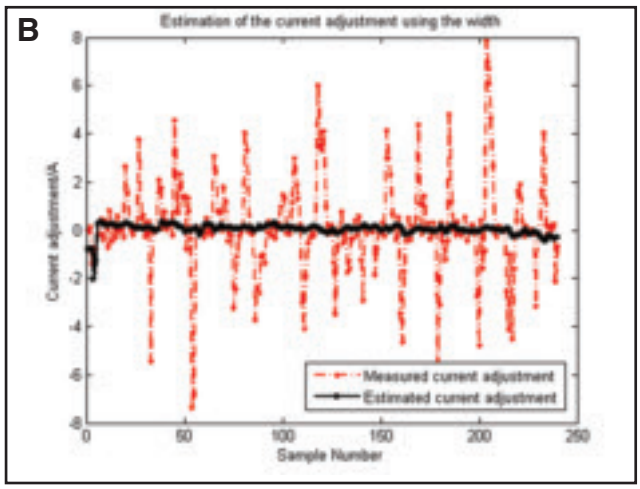

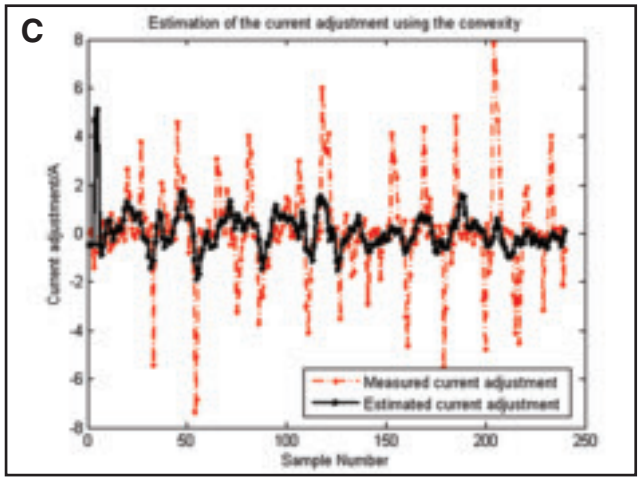

Fig. 3 — Estimation of the welder's response using the models with the single input. A — Estimation using the length; B — estimation using the width; C — estimation using the convexity.

convexity rises.

Figure 2 shows the backside weld bead obtained from the identification experiment. The weld bead width varies approximately periodically. That indicates the human welder did not adjust the current fast and accurately enough to compensate for the effect of the welding speed change on the weld pool geometry. It needs to point out that this is, of course, not required because not every skilled welder could even control the weld bead constant under frequent and substantial changes in the welding speed. In this study, this type of variation is produced on purpose in order to identify how the welder responds to the dynamic weld pool surface.

Identification Method

In the last section, the design of the dynamic experiments is detailed, and experiments are conducted. Before the welder response is modeled using data from these experiments, the methods for model establishment used in the field of system identification (Refs. 2, 3) from experimental data are introduced in this section.

System identification has been studied for many years and is now a standard method to extract dynamic models (Refs. 2, 3). It can be classified into two categories, i.e., continuous time and discrete time. Human welders always scan the weld pool with a certain frequency during the welding process, and the more skilled the human welder is, the slower frequency of scan is needed. Therefore, it is reasonable to apply discrete identification methods in this study to identify the model of the human welder's behavior. To determine the data acquisition frequency, the scan frequency of a human welder can be considered as a reference. In this study, the data acquisition frequency selected is 2 Hz.

Model Structure

In this study, the characteristic parameters selected to describe the front-side weld pool geometry are the width (w), length (l), and convexity (h). That is,

$$\Omega = [w \quad l \quad h]' \qquad (1)$$

According to the principle of a human welder's behavior detailed in Part 1 of this study, it is reasonable to assume that a welder would control the welding process such that the geometric parameter set Ω approaches to the desired dimension Ω*:

$$\Omega^* = [w^* \quad l^* \quad h^*]' \qquad (2)$$

where w^*, l^*, and h^* are the desired parameters for the width, length, and convexity, respectively. In this sense, the adjustment on the current (i.e., the current adjustment, Δi) made by the welder at the present instant k is to bring Ω close to Ω* intuitively, the welder makes the adjustment based on the difference of his newest observation $\Omega(k-d-1)$ (the delay is included) from Ω*:

$$\Delta i(k) = g(1)\big(\Omega(k-d-1) - \Omega^*\big) + e(k) \qquad (3)$$

where $g(1) = [g_1^w, g_1^l, g_1^h]$ is the gain vector, and $e(k)$ is the error. More generally, a welder with a minimal skill should not

Table 2 — Resultant Models of the Human Welder Response with Two Inputs

Inputs	σ	r	Models
Length + Width	1.8994	0.14	$\Delta i_k = -0.0181l_{k-4} - 0.4124l_{k-5} + 0.8868l_{k-6} + 0.0316w_{k-4} + 0.6415w_{k-5} - 0.6716w_{k-6} - 2.041$
Width + Convexity	1.7406	0.418	$\Delta i_k = -0.7345w_{k-2} + 0.71w_{k-3} - 0.9675w_{k-4} + 0.9814w_{k-5} + 43.7353h_{k-2} - 35.8699h_{k-3} + 51.3075h_{k-4} - 54.2302h_{k-5} - 0.5067$
Length + Convexity	1.7239	0.436	$\Delta i_k = -1.1.902l_{k-2} + 1.6078l_{k-3} - 2.0024l_{k-4} + 1.4957l_{k-5} + 55.3252h_{k-2} - 66.1454h_{k-3} + 79.8977h_{k-4} - 66.0899h_{k-5} + 0.1113$

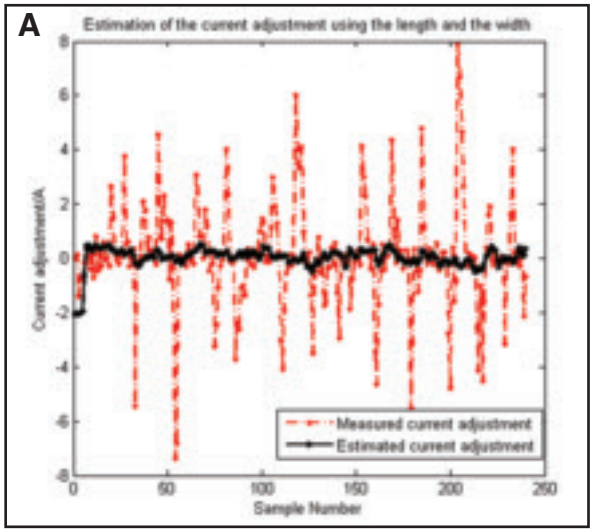

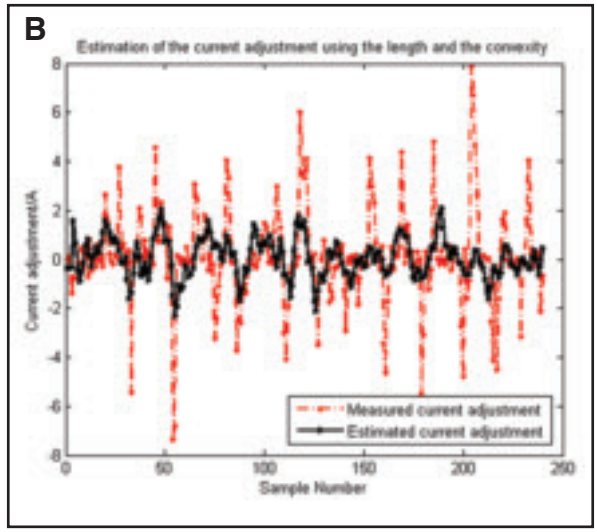

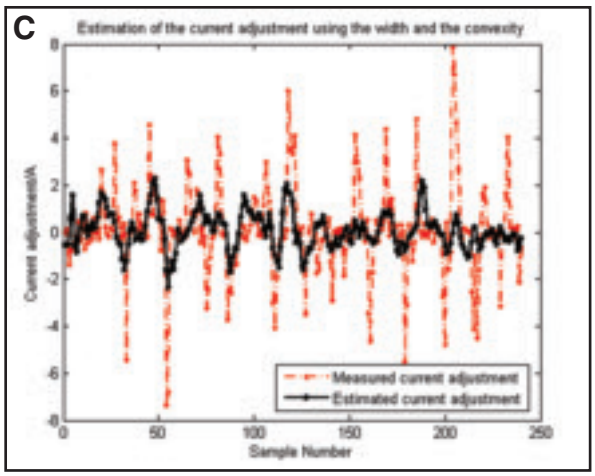

Fig. 4 — Estimation of the welder's response using the models with two inputs. A — Estimation using the length and width; B — estimation using the length and convexity; C — estimation using the width and convexity.

make the adjustment $\Delta i(k)$ only based on the newest difference (delay is included again) but also based on additional previous differences as follows:

$$\Delta i(k) = \sum_{j=1}^{M} g(j)(\Omega(k-d-j)-\Omega^*) + e(k) \quad (4)$$

where $g(j) = [g_j^w, g_j^l, g_j^h]'s$, $j = 1, 2, ...M$ are the gain vectors, and M is the order of the response model. Because Ω^* is a constant vector, model (4) gives

$$\Delta i(k) = \sum_{j=1}^{M} g(j)\Omega(k-d-j) + \Gamma + e(k) \quad (5)$$

where Γ is a constant

$$\Gamma = -\sum_{j=1}^{M} g(j)\,\Omega^* \quad (6)$$

Identification Method

To estimate gains from experimental data, Model 5 can be rewritten as

$$\Delta i(k) = \theta_{M,d}\,\varphi_{M,d}(k) + e(k) \quad (7)$$

where

$$\theta_{M,d} = (\Gamma, g(1), g(2),..., g(M)) \quad (8)$$

$$\varphi_{M,d}(k) = (1, \Omega(k-d-1)', \Omega(k-d-2)',...,\Omega(k-d-M)')' \quad (9)$$

Identification of the human welder's response model is to estimate $\theta_{M,d}$ from the experimental data $\{\Delta i(k), \varphi_{M,d}(k)\}$'s $(k = d + M + 1, d + M + 2, ..., N)$. The most popular parameter estimation method is the least squares algorithm (Refs. 4–6) that minimizes the sum of the squared model errors as follows:

$$J(\hat{\theta}_{M,d}) = \min_{\hat{\theta}_{M,d}} \sum_{k=d+M+1}^{N} \left(\Delta i(k) - \hat{\theta}_{M,d}\varphi_{M,d}(k)\right)^2 \quad (10)$$

to produce the least square estimate $\hat{\theta}_{M,d}$. The standard least squares algorithm can be used to analytically compute $\hat{\theta}_{M,d}$ and the corresponding $J(\hat{\theta}_{M,d})$ from the data $\{\Delta i(k), \varphi_{M,d}(k)\}$'s $(k = d + M + 1, d + M + 2, ..., N)$. For a given model order M and response delay d, its number of parameters in $\hat{\theta}_{M,d}$ is known.

Identification of the human welder's response model is as follows: 1) for a given number of parameters, use the least squares algorithms to calculate all possible models (with different M and d) and corresponding sums of the squared model errors, and then select the one with the minimal sum of the squared model errors as the model for this number of parameters; 2) increase the number of parameters and use the F test (Ref. 7) to determine if the resultant reduction in the sum of the squared errors due to this increase is significant; 3) if significant, increase the number of parameters again; otherwise, the model before the increase gives the identified model. Once the model is finally selected/identified, its accuracy is measured by the standard deviation

$$\sigma = \sqrt{J\left(\hat{\theta}_{M,d}\right)/\left(N-d-M\right)} \quad (11)$$

A time delay has been proposed because of the neuromuscular and central nervous latencies. The existence of this time delay has been verified and estimated in the first part of the paper. It should be noted that this time delay varies according to the physical health/mental conditions, skill level of the human welder, and other human-dependent and environmental factors. It might vary from time to time during the same welding process. Further, the delays for the three weld pool surface characteristic parameters might not be exactly the same. Also, it might not be an integer in the discrete-time model (Ref. 8). However, it can be approximated to an integer, which can be determined through the model identification process as aforementioned in the proposed identification method.

Modeling of Response to Weld Pool Surface

Modeling

With the introduction of model structure and identification method in the last section, the modeling of a human welder's response from the experimental data is conducted in this section.

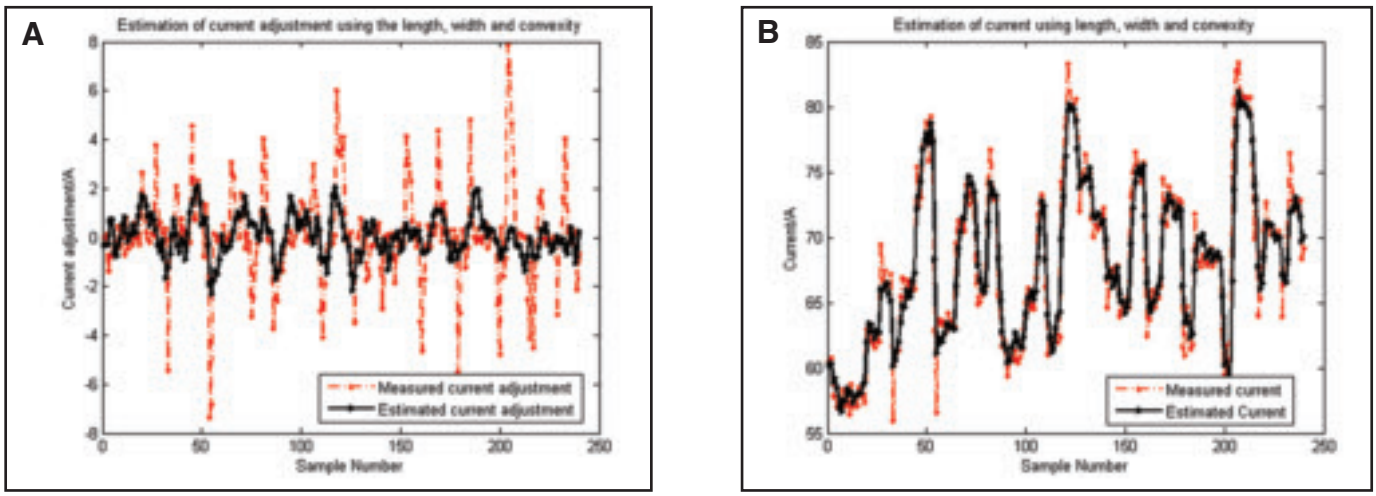

Fig. 5 — Estimation of the welder's response using the models with three inputs. A — Estimation of current adjustment; B — estimation of current.

A subset of the three characteristic parameters may be used to model a human welder's response first to see if all of the three parameters are needed. Using the data shown in Fig. 1 and the identification method given in the previous section, three models in Table 1 that only use one of the three characteristic parameters are first identified. The current adjustments estimated using the resultant models are shown in Fig. 3. Correlation coefficient r in Table 1 measures the strength and direction of a linear relationship between measured and estimated output (Δi) in this study (Ref. 9). The model with a higher accuracy is expected to obtain a higher correlation coefficient. Figure 3 and Table 1 show that the model using the convexity as its input obtains the smallest standard deviation and the highest correlation coefficient. It is because the convexity of the weld pool, when the arc pressure is given, reduces as the backside weld pool width increases because a greater backside weld pool width allows more liquid metal to be pushed from the front surface of the weld pool.

As can be seen from Fig. 3 and Table 1, none of the three models in Table 1 matches the estimated current adjustments well with the measured ones. This indicates that the human welder's response might depend on more than one characteristic parameter of the weld pool surface. Hence, models with more inputs are identified.

The resultant models with two input parameters are presented in Table 2. The current adjustments estimated using the resultant models are shown in Fig. 4.

According to the models in Table 2, the human welder adjusts the current based on the weld pool surface 1 to 3 s ago. Also, the two models using the convexity as one of their inputs better modeled the welder's response. However, the two models that used the convexity show no significant differences in terms of the standard deviation or correlation coefficient. It is probably because the welding speed has a significant effect on the weld pool size, but a slight impact on the weld pool appearance, i.e., the length-to-width ratio does not vary significantly. That means the width and length fluctuate approximately proportional during our experiment that changes the welding speed to change the weld pool.

The resultant model with all three geometric parameters is shown in Equation 12. The standard deviation of model in estimating the current adjustment is 1.713, which is smaller than those of the three models with two inputs shown in Table 2, and the correlation coefficient is 0.448. The current adjustments estimated using the resultant models are shown in Fig. 5A. Figure 5B is the comparison between the measured current and estimated current obtained by the model.

$$\begin{aligned}\Delta i_k = &-1.3066 l_{k-2} + 2.4704 l_{k-3} \\ &- 3.1688 l_{k-4} + 1.8859 l_{k-5} - 0.8893 w_{k-3} \\ &+ 0.9658 w_{k-4} + 0.5371 w_{k-5} - 0.6277 w_{k-6} \\ &+ 55.2372 h_{k-2} - 63.4404 h_{k-3} \\ &+ 90.8986 h_{k-4} - 96.1477 h_{k-5} \\ &+ 17.5644 h_{k-6} + 0.2077 \end{aligned} \quad (12)$$

Table 3 — ARX Models of the Human Welder Response

Inputs	σ	r	Models
Length + Width + Convexity	1.5722	0.571	$\Delta i_k - 0.4725\Delta i_{k-1} + 0.1366\Delta i_{k-2} = 0.6097 l_{k-3} - 2.2283 l_{k-4} + 1.6137 l_{k-5} - 1.2675 w_{k-3} + 1.7667 w_{k-4} + 0.0930 w_{k-5} - 0.6088 w_{k-6} + 30.3658 h_{k-3} + 19.6357 h_{k-4} - 67.6373 h_{k-5} + 18.7761 h_{k-6}$

Table 4 — Z-Transfer Functions of the ARX Model

Model	z-transfer function
Length + Width + Convexity	$A'_{lwh}(z) = z^3 (z^2 - 0.4725z + 0.1366)$
	$A''_{lwh}(z) = z^4 (z^2 - 0.4725z + 0.1366)$
	$B_l^{lwh}(z) = 0.6097z^2 - 2.2283z + 1.6137$
	$B_w^{lwh}(z) = -1.2675z^3 + 1.7667z^2 + 0.0930z - 0.6088$
	$B_h^{lwh}(z) = 30.3658z^3 + 19.6357z^2 - 67.6373z + 18.7761$

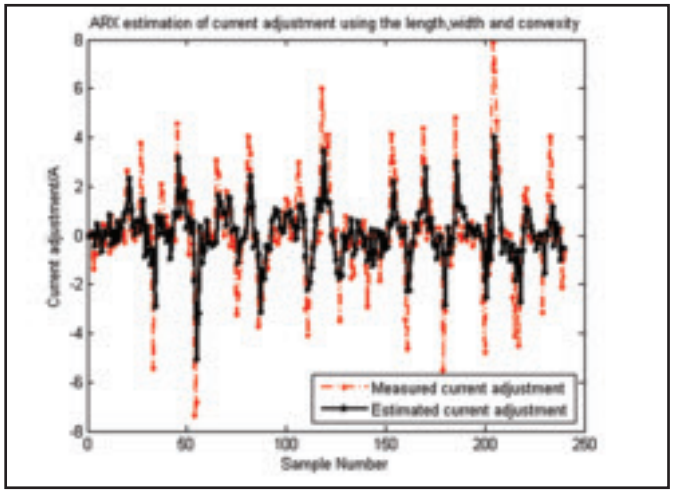

Fig. 6 — Estimation of the welder's response using the ARX model that uses all three characteristic parameters.

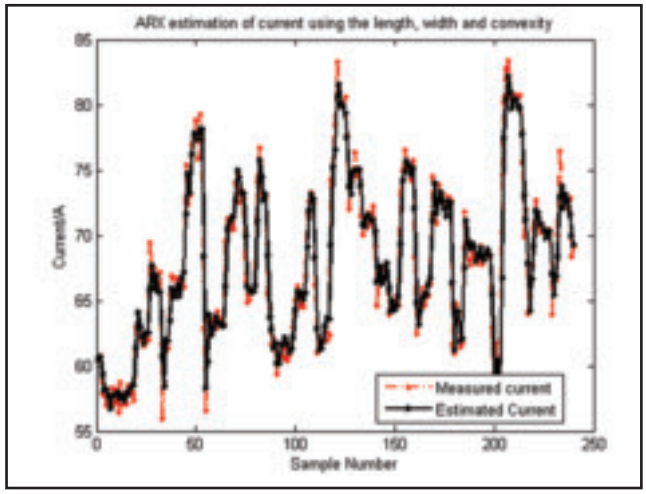

Fig. 7 — Comparison of the ARX model estimated welding current with the measured current. The ARX model makes use of the width, length, and convexity calculated from the 3D weld pool surface as the weld pool characteristic parameters, and the previous adjustments on the welding current to predict the welder's adjustment on the welding current.

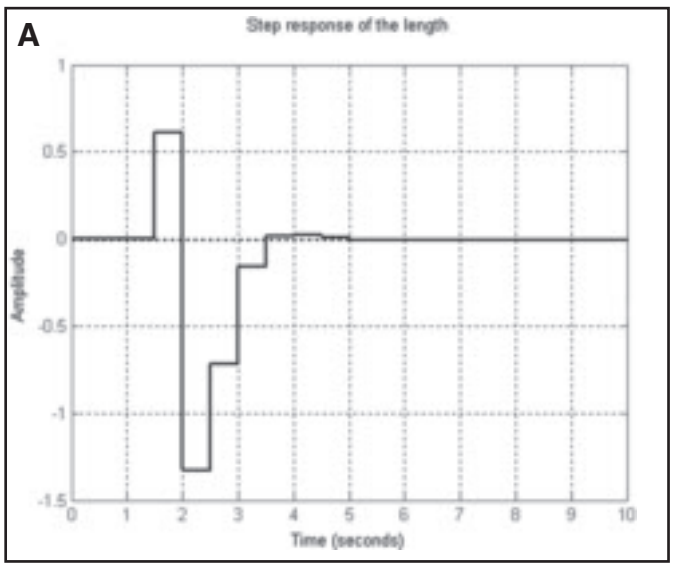

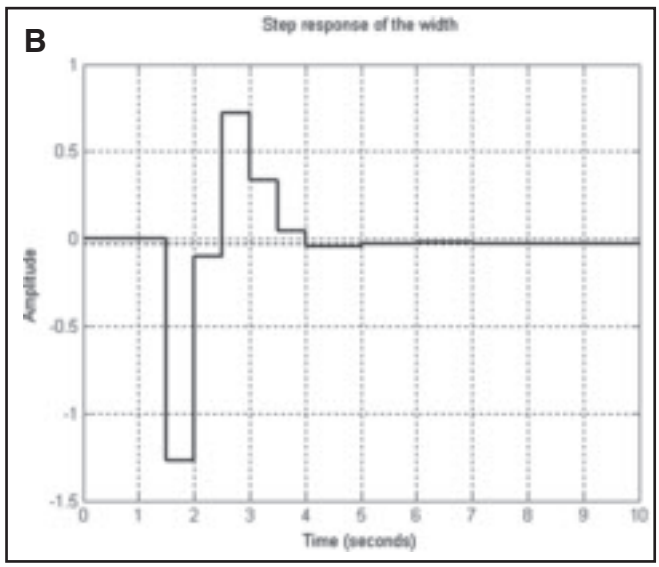

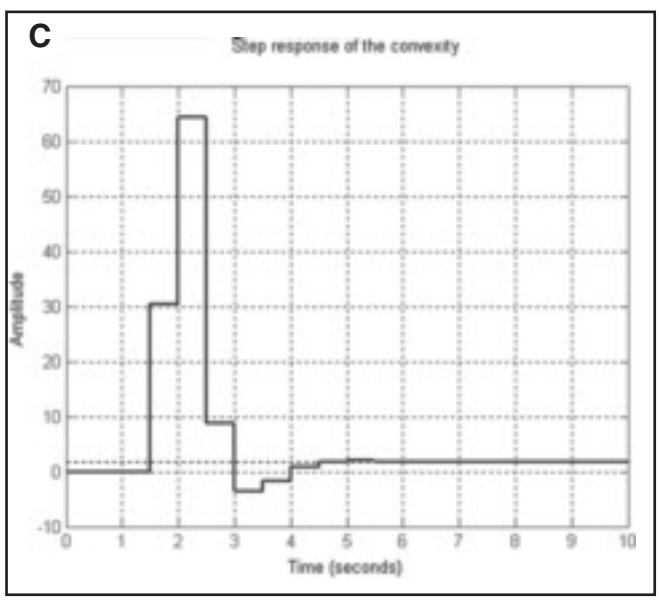

Fig. 8 — Step responses of the ARX model. A — Length step response; B — width step response; C — convexity step response. Because the output is Δi, all the step responses settle down back to approximately zero. The integration of the step response gives the net change in the welding current due to the step change in one of the characteristic parameters. In A, the integration is negative. This implies that the welder reduces the current as a response to an increased weld pool length. In B, the integration is negative. The welder again reduces the current as a response to an increased weld pool width. In C, the integration is positive. The welder increases the current as a response to an increased convexity.

Static Response Analysis

A human welder always tries to control the state of the welding process approaching the desired state, and the desired state of the weld pool geometry is contained in the constant of the model in Equation 5. The desired state Ω^* can be obtained by solving the static state equations of the models in Tables 1 and 2. The static state equation of the model using the convexity as the input is shown in Equation 13. The static state equations of the last two models in Table 2 are shown, respectively, in Equations 14 and 15.

$$\Delta I = 4.2284H - 0.4715 \quad (13)$$

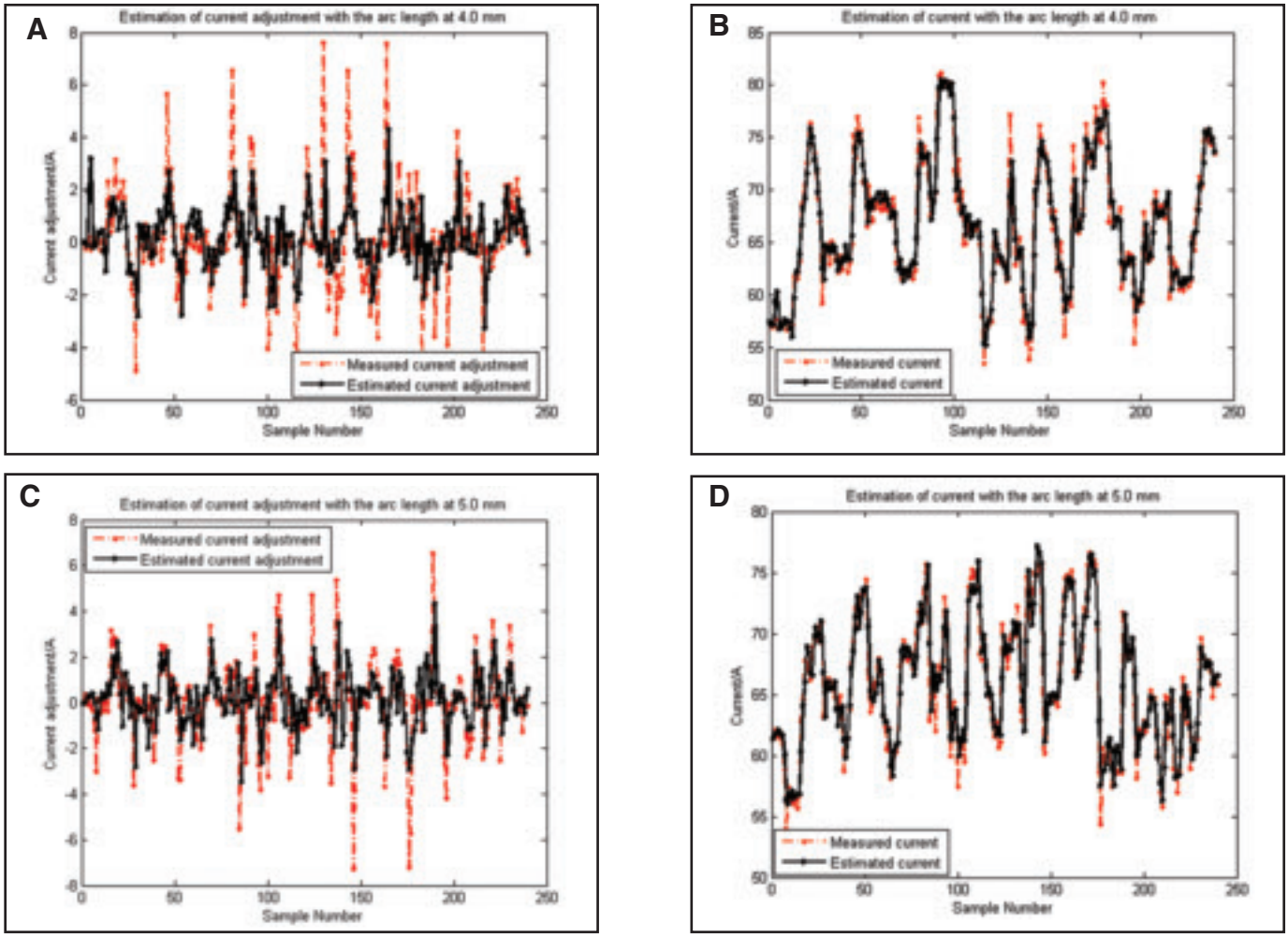

Fig. 9 — The prediction of the human welder's response using model H_{lwh} (z). A — Estimation of current adjustment with arc length 4.0 mm; B — estimation of current with arc length 4.0 mm; C — estimation of current adjustment with arc length 5.0 mm; D — estimation of current with arc length 5.0 mm.

$$\Delta I = -0.0106W + 4.9427H - 0.5067 \quad (14)$$
$$\Delta I = -0.0891L + 2.9876H + 0.1113 \quad (15)$$

where ΔI is the current adjustment at static state; W, L, and H are the width, length, and convexity of the weld pool at static state. As the welding process approaches the desired state assessed by the human welder, the welder stops changing the current. The current adjustment equals zero. In this sense, the W, L, and H are the desired state of the weld pool geometry, i.e., $W = w^*$, $L = l^*$, and $H = h^*$. Solving Equations 13 to 15, the resultant desired state Ω^* is as follows:

$$\Omega^* = [4.1934 \quad 4.9933 \quad 0.1115]' \quad (16)$$

It is reasonable for the human welder to choose the set of the geometric parameters as the desired state given the specific settings for the experiment detailed in the previous experimental method section. It can be seen in Fig. 2, the backside weld bead width varies greatly during the process since the welder does not perform well enough to keep the width consistent. However, it is an indication of the welder's skill in execution of the current output, and irrelevant to the desired state the human welder wants to maintain. Also, the desired state of weld pool geometry can be verified by estimating the constant in the model with the three inputs shown in Equation 12. The static state equation of the model can be written in the following equation:

$$\Delta I = -0.1191L - 0.0141W + 3.8121H + 0.2077 \quad (17)$$

Substituting Equation 16 into 17, and letting $\Delta I = 0$, the estimated constant in Equation 14 is obtained as the following:

$$\Gamma = 0.2287 \quad (18)$$

The estimated value matches the value in the model with a 0.021 difference, which may be caused by the accuracy of the model in predicting the human welder's response. Also, the disturbance/noise during the data-acquisition process might contribute some of the difference. Further, it is found that the estimated constants coincide with constants in the mod-

Table 5 — Poles and Zeros of the ARX Model

Inputs	Poles and zeros
Length + Width+ Convexity	$A'_{lwh}(z)$: [0.2363±0.2842i, 0,0,0], $A''_{lwh}(z)$: [0.2363±0.2842i, 0,0,0,0] $B_{l\ lwh}(z)$: [0.9952, 2.6596], $B_{w\ lwh}(z)$: [–0.52, 0.9571±0.0823i] $B_{h\ lwh}(z)$: [–1.9509, 0.9812, 0.323]

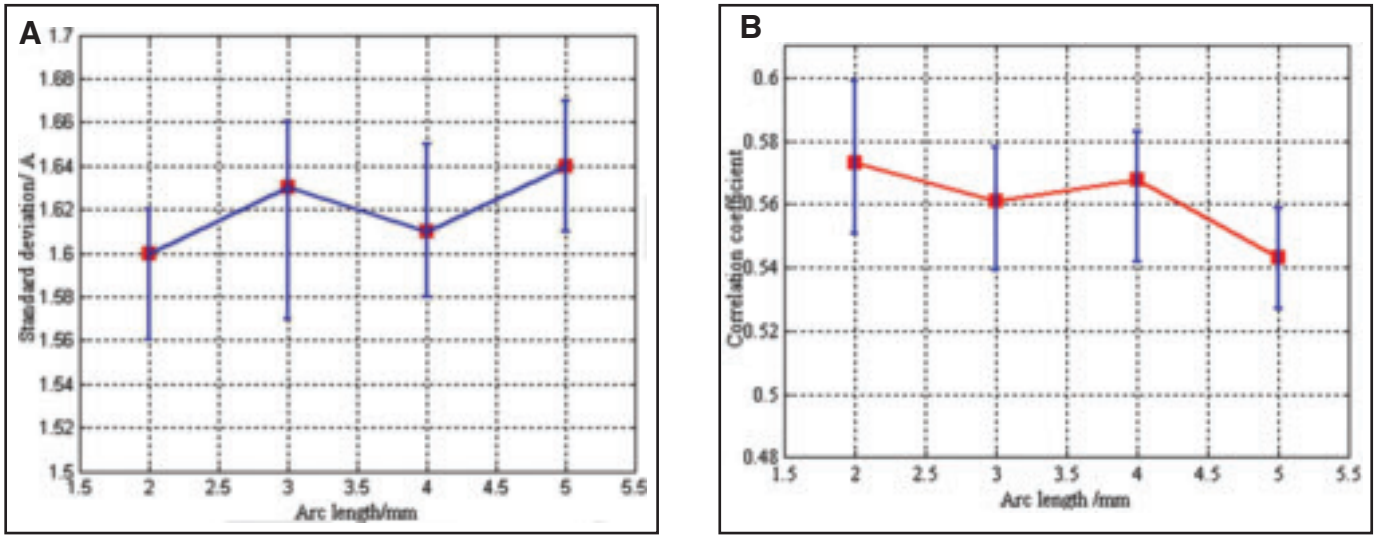

Fig. 10 — Standard deviations and correlation coefficients of the model using data from the verification experiments at different arc lengths. A — Standard deviation of the model; B — correlation coefficients of the model.

els listed in Tables 1 and 2.

Furthermore, according to the static state equation of the model shown in Equation 17, the human welder tends to reduce the current as the length or width grows, and increases the current as the convexity of the weld pool rises. The coefficient of the width in the model is smaller than other coefficients in the model, while the convexity has the largest coefficient in the model. That indicates the welder is more sensitive to the convexity and length, and less sensitive to the width of the weld pool during the welding process.

Improved Modeling and Understanding of Human Welder Response

Although the model with all three characteristic parameters is more accurate than those with less characteristic parameters in predicting the welder's responses, the estimated current adjustment still does not quite well fit the measured one. To better understand and predict the welder's behavior, let's analyze below.

The following model, referred to as the auto-regressive with exogenous terms (ARX) model, is the general structure to describe discrete-time linear systems:

$$y(k) = a(1)y(k-1) + \ldots + a(M_1)y(k-M_1) + b(1)u(k-d-1) + \ldots + b(M_2)u(k-d-M_2) + e(k) \quad (19)$$

where u is the input, y is the output, d is the delay, e is the disturbance, and $a(l)$, ($l = 1, \ldots, M_1$), $b(j)$, ($j = 1, \ldots, M_2$) are the model parameters of the system. The MA (moving-average) model

$$y(k) = b(1)u(k-d-1) + \ldots + b(M_2)u(k-d-M_2) + e(k) \quad (20)$$

is one of its simplified structure. It may adequately describe certain discrete-time dynamic processes but not all discrete-time dynamic processes. The model in Equation 5, intuitively proposed based on our analysis and understanding of a human welder's response, is apparently an MA model with Ω as the inputs and Δi as the output. Its less than ideal accuracy may have been caused by its inadequacy in describing the human welder's dynamic response process. If this is the case, use of the more general ARX model structure may improve the model accuracy significantly and help us better understand the behavior of the human welder.

Based on the above analysis, the following ARX model structure is proposed to improve the modeling accuracy for the human welder's response:

$$\Delta i(k) = \sum_{l=1}^{M_1} a(l)\Delta i(k-l) + \sum_{j=1}^{M_2} b(j)\,\Omega\,(k-d-j) + e(k) \quad (21)$$

The inclusion of $\Delta i(k-1), \ldots, \Delta i(k-M_1)$ into the model basically introduces the welder's previous actions. If this inclusion can better predict the welder's adjustments on the welding current, it would suggest that the welder not only depends on the weld pool surface but also on his previous actions to adjust the welding current. Our understanding of the human welder's behavior would be improved.

The parameter estimation and model structure identification for ARX models are similar as those for MA models and standard in the system identification literature (Refs. 10–12). Since all three characteristic parameters are found necessary, the ARX models with all three characteristic parameters are identified. The resultant model is listed in Table 3, and the model results are shown in Figs. 6 and 7. As can be seen from Table 3, the present adjustment at instant k on the current Δi_k depends on the characteristic parameters 3 through 6 periods previously, i.e., $k-3$ to $k-6$. Hence, the welder makes an adjustment on the current based on the weld pool he observed approximately 1.5 to 3 s previously. There is a difference from 1 to 3 s given by the less accurate intermediate model in Table 2, but this difference is considered insignificant.

As can be seen, in general, the ARX model well matches the estimated current adjustments to the measured current adjustments except a few current peaks — Fig. 6. The ARX model is much better than the MA models in Table 2 for predicting the human welder's response. That indicates the human welder's adjustment on the current does also depend on his previous responses/actions. Figure 7 shows the comparison between the measured current and estimated current using the ARX model. Since the experiment is conducted by a newly trained welder for this study who may frequently overreact/underreact during the operation, it is understandable that the steep current adjustments cannot, and should not, be fit well using the model. A model can possibly better estimate the skilled human welder's response with fewer sudden current changes and randomness in the welding process.

In order to analyze the model's properties, the ARX model is written in z-transfer functions (Ref. 13), shown in Table 4. The poles and zeros of the z-transfer function are listed in Table 5.

It can be seen that all the poles of the

model are inside the unit circle in Z-plane, which means that the model as the controller in Table 4 is asymptotically stable (Ref. 14), which is easily understood. In fact, the human welder makes the adjustment on the welding current as an intelligent controller. This controller can and should be able to deliver a stable welding process despite his limited experience training. Hence, the model for the welder's response should be stable. Further, there is only one pair of conjugate poles. The oscillation frequency of the transition responses is

$$\omega_{lwh} = 1.7543 \text{ rad/s} \qquad (22)$$

The settling time for the unit step response is approximately 4 s, as can be seen in Fig. 8. Because the welding process is dynamic, the transition time discussed in the first part of the paper is approximately the sum of the settling times for the controller and welding process. It is much longer than that of the controller, which is approximately 4 s as discussed above.

Another characteristic of the model is that it is a nonminimum phase system (Ref. 15), since there are zeros outside the unit circle in Z-plane as shown in Table 5. Per literature (Refs. 16, 17), this often leads to relatively large overshoot/undershoot. Such oscillations can be observed from the simulated step responses shown in Fig. 8. It is suspected that the model for a skilled/experienced welder would exhibit much less significant oscillations.

Verification and Discussion

Due to the consistency of the human welder's performance, the obtained model should have a similar performance to predict the current in other experiments. To further verify the model, the verification experiments are designed and conducted as discussed in the experimental method section. To produce an acceptable distribution of the welding parameters to ensure the validity of the resultant model, each experiment is conducted at a constant arc length in [2, 5 mm], i.e., 2, 3, 4, and 5 mm. For each arc length setting, there are five experiments conducted with the random welding speed signal.

Figure 9 shows the estimated current/current adjustment obtained by the model using the data from two of the verification experiments under different arc lengths. It can be seen that the estimated current adjustments predict all the tendencies of the measured current adjustments, although there are some high and steep measured values at which the estimation cannot follow in magnitude. Moreover, the curves of the estimated and measured current coincided well.

The standard deviation and correlation coefficient are the criteria to evaluate the performance of the model when applied to different verification experiments. All the standard deviations and correlation coefficients obtained for the model to estimate the current adjustments in the verification experiments are shown in Fig. 10A and B, respectively. The square and error bar for the experiments at each arc length in the figures are the mean value and the range of the two values is from the verification experiments conducted at this particular arc length. The average standard deviation is about 1.6 A. The correlation coefficients at the different arc lengths in Fig. 9 vary almost within the same range around their mean values. The average correlation coefficient of all the verification experiments is about 0.56. However, the mean correlation coefficient at arc length 5 mm is smaller than that in the other three arc lengths. It is possibly because as the arc length increases, the current required for the same penetration state is higher. Then, during the experiments, the human welder needs to adjust the current in a large range. That might have increased inaccuracy in predicting the current adjustments using the model. Other than that, the model shows a consistent performance in predicting the human welder's response on the adjustment of the current during the verification experiments.

Conclusion

This paper modeled adjustments on the welding current made by a human welder in response to the 3D weld pool surface, as characterized by its length, width, and convexity, to maintain a consistent complete joint penetration in gas tungsten arc welding (GTAW). The dynamic changes in the weld pool surface were produced by conducting experiments using randomly changed welding speeds from 1.00 to 2.00 mm/s. Under the experimental conditions used, the following were found:

- The human welder makes the adjustment on the welding current based on the current and previous weld pool surfaces.
- The adjustment on the welding current by the human welder requires the length, width, and convexity of the weld pool surface to model adequately. From the established model, the human welder responds to the weld pool surface he observed approximately 1.5 to 3 s previously.
- The human welder makes the adjustment on the welding current also based on the previous adjustments he has made 1 s prior.

It is noted from the identification and verification results that the adjustments on the welding current cannot be fully predicted. This is expected because of the relatively limited skills of the novice human welder and the inconsistency of his operation/concentration. The modeling errors are a reflection of the human welder's skill level and concentration.

Acknowledgments

This work is funded by the National Science Foundation under grant CMMI-0927707. We wish to thank Yi Lu and Yukang Liu for their assistance on experiments and graphics, and Lee Kvidahl for his technical guidance on manual pipe welding.

References

1. Zhang, W. J., and Zhang, Y. M. 2012. Modeling of human welder response to 3D weld pool surface: Part I – Principles. *Welding Journal* 91(11): 310-s to 318-s.

2. Wickens, C. D., and Carswell, C. M. 1997. Information processing. *Handbook of Human Factors and Ergonomics.* Ed. Salvendy, G. New York: Wiley.

3. Kerschen, G., Worden, K., Vakakis, A. F., and Golinval, J. C. 2006. Past, present, and future of nonlinear system identification in structural dynamics. *Mechanical Systems and Signal Processing* 20: 505–592.

4. Scharf, L. 1991. *Statistical Signal Processing*. Reading, Mass.: Addison-Wesley.

5. Haykin, S. 1996. *Adaptive Filter Theory,* Third Edition. Englewood Cliffs, N.J.: Prentice-Hall.

6. Kailath, T., Sayed, A., and Hassibi, B. 2000. *Linear Estimation*. Englewood Cliffs, N.J.: Prentice-Hall.

7. Richard, G. L. 2007. *Statistical Concepts: A Second Course,* Third Edition. Routledge Academic.

8. Boer, E. R., and Kenyon, R. V. 1998. Estimation of time-varying delay time in non-stationary linear systems: An approach to monitor human operator adaptation in manual tracking tasks. *IEEE Transactions on Systems Man and Cybernetics Part A-Systems and Humans* 28(1): 89–99.

9. Edwards, A. L. 1976. *An Introduction to Linear Regression and Correlation*. San Francisco, Calif.: W. H. Freeman.

10. Ljung, L. 1999. *System Identification — Theory for the User,* 2nd edition. Upper Saddle River, N.J.: PTR Prentice Hall.

11. Juang, J. 1994. *Applied System Identification*. Upper Saddle River, N.J.: Prentice Hall.

12. Söderström, T., and Stoica, P. 1989. *System Identification*. Upper Saddle River, N.J.: Prentice Hall.

13. Cornelius, T. L. 1996. Digital control systems implementation and computational techniques. Academic Press.

14. Chen, C. T. 1999. *Linear System Theory and Design,* 3rd Edition. Oxford University Press.

15. Hassibi, B., Kailath, T., and Sayed, A. H. 2000. Linear estimation. Englewood Cliffs, N.J.: Prentice Hall.

16. Hoagg, J. B., and Bernstein, D. S. 2007. Non-minimum phase zeros — Much to do about nothing. *IEEE Control System Magazine* 27(3): 45–57.

17. Lau, K., Middleton, R. H., and Braslavsky, J. H. 2003. Undershoot and settling time tradeoffs for non-minimum phase systems. *IEEE Transactions on Automatic Control* 48(8): 1389–1393.